A Unified Approach for Multi-Granularity Search over Spatial Datasets

Wenzhe Yang
Wuhan University
wenzheyang@whu.edu.cn

Sheng Wang*
Wuhan University
swangcs@whu.edu.cn

Shixun Huang
The University of Wollongong
shixun_huang@uow.edu.au

Yuyang Liao
Wuhan University
yuyangliao@whu.edu.cn

Yuan Sun
La Trobe University
yuan.sun@latrobe.edu.au

Juliana Freire
New York University
juliana.freire@nyu.edu

Zhiyong Peng
Wuhan University
peng@whu.edu.cn

arXiv:2412.04805v3 [cs.DB] 26 Apr 2025

Abstract

There has been increased interest in data search as a means to find relevant datasets or data points in data lakes and repositories. Although approaches have been proposed to support spatial dataset search and data point search, they consider the two types of searches independently. To enable search operations ranging from the coarse-grained dataset level to the fine-grained data point level, we provide an integrated one that supports diverse query types and distance metrics. In this paper, we focus on designing a multi-granularity **spa**tial **da**ta **s**earch system, called Spadas, that supports both dataset and data point search operations. To address the challenges of the high cost of indexing and susceptibility to outliers, we propose a unified index that can drastically improve query efficiency in various scenarios by organizing data reasonably and removing outliers in datasets. Moreover, to accelerate all data search operations, we propose a set of pruning mechanisms based on the unified index, including fast bound estimation, approximation technique with error bound, and pruning in batch techniques, to effectively filter out non-relevant datasets and points. Finally, we report the results of a detailed experimental evaluation using six spatial data repositories, achieving orders of magnitude faster than the state-of-the-art algorithms and demonstrating the effectiveness by case study. An online spatial data search system of Spadas is also implemented and made accessible to users.

PVLDB Reference Format:
Wenzhe Yang, Sheng Wang*, Shixun Huang, Yuyang Liao, Yuan Sun, Juliana Freire, and Zhiyong Peng. A Unified Approach for Multi-Granularity Search over Spatial Datasets. PVLDB, 19(X): XXX-XXX, 2026.
doi:XX.XX/XXX.XX

1 Introduction

The development of sensor technology, GPS-enabled mobile devices, and wireless communication brings prosperity to spatial data, and the emergence of a large number of spatial data has fueled the demand for searching spatial data [16, 27, 28, 45, 62, 70, 78]. Since a spatial dataset usually consists of a set of spatial data points [70], various spatial *dataset* search [41, 42, 70] and *data point* search systems [9, 22, 29] have been developed. For example, Foursquare [9] helps users find the best location points in any city around the world. OpenStreetMap [8] provides search functionality over a vast collection of spatial datasets contributed by users worldwide. However, these systems primarily support keyword-based searches limited to published dataset metadata [19, 23, 82].

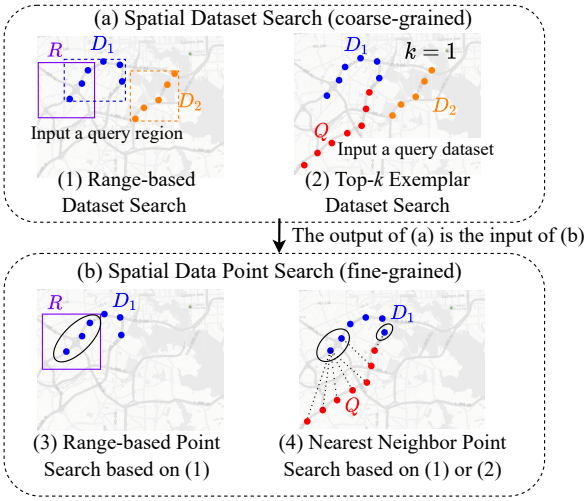

Figure 1: The illustration of our multi-granularity search research over spatial datasets, which seamlessly integrates the dataset search (including (1) and (2) based on three distance metrics) and data point search (including (3) and (4)).

The published spatial metadata is often missing or incomplete [1], rendering keyword-based queries insufficient for helping users locate datasets or data points. Therefore, various query operations that rely on raw data have been developed to identify spatial datasets and data points. For example, existing spatial dataset search engines treat a dataset as the smallest return unit. In contrast, in the existing spatial data point search engines, a data point is the smallest return unit. In what follows, we use a traffic analysis example to introduce these two types of searches.

Example 1. *Consider a scenario where traffic analysts want to analyze traffic patterns in a metropolitan area. Firstly, they can define a query range of R [1, 17, 78] to locate all relevant traffic datasets within that area for analysis, as illustrated on the left side of Figure1(a). Then, to identify the most efficient commuting routes, the analysts can input a specific traffic dataset Q and search for datasets similar to*

This work is licensed under the Creative Commons BY-NC-ND 4.0 International License. Visit https://creativecommons.org/licenses/by-nc-nd/4.0/ to view a copy of this license. For™ any use beyond those covered by this license, obtain permission by emailing info@vldb.org. Copyright is held by the owner/author(s). Publication rights licensed to the VLDB Endowment.

Proceedings of the VLDB Endowment, Vol. 19, No. X ISSN 2150-8097.
doi:XX.XX/XXX.XX

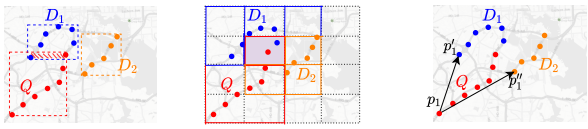

(a) Intersecting area (IA) (b) Grid-based overlap (GBO) (c) Hausdorff distance (Haus)

Figure 2: The illustration of three distance metrics, where (a) shows that the IA of Q and D_1 is the size of their minimum bounding rectangles' overlapping areas, i.e., the rectangle filled with red lines, (b) shows that the GBO of Q and D_1 is 1 since there is one overlapping cell between Q and D_1, and (c) shows that the Haus of Q and D_1 is the maximum nearest neighbor distance, i.e., the distance from the point p_1 of Q to the point p'_1 of D_1.

Q based on defined similarity measures [65, 66, 70] for data analysis, illustrated on the right side of Figure 1(a). This search manner is known as exemplar search [41, 44, 55, 64, 71, 73]. Furthermore, if the analysts want to find points of interest, such as gas stations or rest areas along the searched routes D, they can specify a query range R along with the relevant traffic dataset to retrieve these points, as depicted on the left side of Fig.1(b)[9, 53, 62, 79]. Additionally, on the right side of Figure1(b), the analysts can identify the nearest gas stations for each location in the dataset Q [25, 26, 29, 53, 79], which helps commuters find convenient stops along their routes [72, 74].

What is the Problem? Despite the efforts made in the field of spatial data search systems, existing systems focus mainly on one type of search. There is currently no system that has successfully integrated all types of searches into a unified search framework. In addition, the existing systems, such as Auctus [1] and OpenStreetMap [8], are relatively simple in spatial data search and do not take into account the similarity measurement of spatial location distribution characteristics. Our study, depicted in Figure 1, considers all searches at both the coarse-grained spatial dataset level and the more fine-grained data point level. In spatial dataset search, we integrate range-based dataset search and top-k exemplar dataset search based on several distance metrics.

As shown in Figure 2, the intersecting area (IA) [28, 39] is useful when assessing the overlap between public transportation routes, which can help identify congestion points to optimize traffic management. Compared to IA, grid-based overlap (GBO) [45] can capture the density of traffic in the urban grid in a finer granularity and optimize traffic routes. In addition, calculating the Hausdorff distance (Haus) [30, 46, 59] can help analysts understand the accessibility of bus stops for residents (the formal definition is in Section 3.2). Moreover, building upon the outcomes of the dataset search, we further enhance our capabilities to facilitate a finer-grained data point search process, wherein the results obtained from the dataset search are fed to the subsequent data point search.

What are the Challenges? Our goal is to design a multi-granularity spatial data search system that seamlessly supports coarse-grained dataset search based on multiple distance metrics and fine-grained data point search. There are several challenges: Firstly, A naïve way is to build separate indexes for each query type. However, this method incurs significant costs in both storage and index construction time. Furthermore, the presence of outliers in spatial datasets, such as erroneous data points caused by GPS errors, can severely affect the accuracy and efficiency of similarity computation [63]. Finally, although the index can quickly locate data matching query criteria, it does not effectively reduce the number of candidate points to examine. Thus, there is an urgent need for efficient acceleration strategies to speed up a rich set of searches.

How the Challenges are Addressed? To address the challenges above, we develop a multi-granularity spatial data search system, called Spadas. Specifically, we design a *unified index* [37, 67] that can effectively organize both datasets and data points, enabling efficient pruning for various search scenarios. In addition, to further enhance system performance, we propose a set of novel and highly efficient *pruning mechanisms*, such as efficient bound estimation or error-bounded approximation techniques, ensuring that irrelevant candidates are filtered early in the process, thereby reducing computational overhead and improving overall system performance. Our main contributions are summarized as follows.

- We propose a multi-granularity spatial data search system, called Spadas, to efficiently support coarse-grained dataset search based on multiple distance metrics and fine-grained data point search (see Section 4). We also implement an online Spadas system[1] that can be accessed by users.
- To support both searches with different query types and distance metrics, we specifically design a unified index to enhance the efficiency of data search operations by efficiently organizing spatial data, while mitigating the influence of outliers on the accuracy of similarity measures between datasets (see Section 5).
- To accelerate multiple types of data search operations, we propose a range of pruning mechanisms over the unified index, including tighter lower and upper bounds, approximation technique with error bound, and batch pruning, that effectively filter candidates and thus significantly reduce computational overhead (see Section 6).
- We conduct extensive experiments on six real-world data repositories, and the results show that our proposed Spadas can achieve orders of magnitude speedup than the state-of-the-art algorithms in dataset search and data point search. The case studies validate the effectiveness of our search system (see Section 7).

2 Related Work

In this section, we give a literature review on spatial dataset search and spatial data point search.

2.1 Spatial Dataset Search

Overlap-based Similarity Search. For a user with a query dataset, the overlap-based similarity search ranks candidate datasets based on the size of their overlap area. Computing the overlapping area between two Minimum Bounding Rectangles (MBRs) is a commonly used and straightforward measure. Frontiera et al. [30] proposed several variants by considering the query and the dataset's range. Vasconcelos et al. [27] and Degbelo et al. [28] applied it as the main ranking metric for an open government dataset search portal. More recently, with the rise of grid partition technology [68, 78], a more fine-grained similarity measure based on the number of overlapping grid cells began to appear, i.e., modeling each dataset as a grid with points inside by dividing the space equally and using the intersection of the grids as the similarity.

[1] http://swangdbs.com/prototype/spadas/

Point Set Similarity Search. Point set similarity search mainly calculates the distance between each pair of points to assess the similarity between two datasets. For instance, Hausdorff distance [12, 24, 28, 31, 43, 46, 59] measures the similarity between two datasets by calculating the maximum distance from any point in one dataset to its nearest point in the other dataset. Specifically, Nutanong et al. [46] derived the lower and upper bounds of Hausdorff and combined them with the branch-and-bound strategy to improve efficiency. Degbelo et al. [28] conducted experiments to verify that the Hausdorff distance has higher precision than the overlapped area in dataset search. However, the complexity of the existing upper and lower bounds is still high, and we need more efficient bound estimation to speed up the Hausdorff computation. In addition, earth mover's distance [41, 42, 70] is a more fine-grained point set similarity measure compared to Hausdorff. However, it is a more expensive distance as it has a cubic time complexity.

2.2 Spatial Data Point Search

Range-based search. As one of the fundamental operators in spatial databases, the goal of range-based search is to find all objects falling within the query region. For example, Hariharan et al. [36] constructs a location-based search engine, which supports users to specify a query range, and then all points that fall into the query region are returned to the users. Zacharatou et al. [78] proposed a spatial bundled dataset search over different domains using spatial ranges. In the spatial dataset search system Auctus [1, 19], range queries are supported by returning spatial datasets that overlap with the user-specified query region. Papadopoulos et al. [50] also studied multiple-range query optimization strategies to improve search efficiency by grouping multiple queries.

k Nearest Neighbor search. The kNN [22, 33, 47, 53, 75] is defined as finding k points in a given set that are closest to a given query point. The kNN queries have been extensively studied in the literature. To find the k closest neighbor for any given query point, we can utilize the fundamental kNN search approach, which is often called the brute force (BF) method. For the given query points, it scans the entire dataset to find the k closest points based on the distances between the query point and all other data points, which is computationally intensive. Thus, to efficiently accelerate the kNN search, a variety of indexes with different heuristic improvements have been proposed, such as R tree [34], K-Dimensional tree (KD-tree) [58], and Ball-tree [48]. While these indexes can be implemented to find k nearest neighbor points for a given point, they cannot support both spatial dataset search and spatial data point search, which is the focus of this work.

Remarks. No work has integrated the above spatial dataset search and data point search. Although there exist some index techniques to speed up the search process, different types of queries usually require a dedicated index structure. They do not consider building a unified index, not to mention pruning mechanisms with the index to accelerate query processing.

3 Definitions

In this section, we first introduce the data model and multiple similarity metrics between spatial datasets. Subsequently, we introduce coarse-grained dataset search and fine-grained data point search, followed by the formalization of the problem of multi-granularity spatial data search.

3.1 Data Model

Definition 1. ***(Spatial Data Point).*** *A spatial data point $p = (x, y, v_1, \cdots, v_{d-2})$ is a d-dimension vector ($d \geq 2$), which has at least a latitude x and a longitude y, and can have $d-2$ other attributes.*

For ease of presentation, we use 2-dimensional points for illustration in the subsequent descriptions. However, all search operations we support can be easily extended to multi-dimensional datasets [51], as shown in Section 7. .

Definition 2. ***(Spatial Dataset).*** *A spatial dataset D contains a set of 2-dimension points, i.e., $D = \{p_1, p_2, \cdots, p_{|D|}\}$, where $|D|$ is the size of D. The minimum bounding rectangle (MBR) of D, whose sides are parallel to the x and y axes and minimally enclose all points, is specified by the bottom left corner $b^{\downarrow}$ and upper right corner $b^{\uparrow}$, i.e.,*

$$D.b^{\uparrow}[i] = \max_{p \in D} p[i], \quad D.b^{\downarrow}[i] = \min_{p \in D} p[i], wrt., i \in \{1, 2\} \tag{1}$$

Definition 3. ***(Spatial Data Repository).*** *A spatial data repository $\mathcal{D}$ is composed of a set of spatial datasets, i.e., $\mathcal{D} = \{D_1, \cdots, D_{|\mathcal{D}|}\}$, where $|\mathcal{D}|$ is the number of datasets in $\mathcal{D}$.*

When measuring the similarity between two datasets, existing systems [27, 28] mainly use the intersecting area between the MBR of datasets to measure the overlap ratio. To enable a more fine-grained measure of overlap, we introduce a structure called *z-order signature* to represent each spatial dataset. Specifically, given an integer θ, we partition the entire space containing the spatial data repository into a grid C_θ of $2^\theta \times 2^\theta$ equally-sized cells [18, 54, 77], where θ is referred to as the *resolution*.

Each cell, denoted as c, can be treated as an element. The coordinates of cell c can be converted into a unique non-negative integer $c.id$ by interleaving the binary representations of its coordinate values [52, 57, 70, 78]. This transformation yields consecutive IDs in the range $[0, 2^\theta \times 2^\theta - 1]$. In this way, a spatial dataset D can be represented as a sorted integer set consisting of a sequence of cell IDs. The formal definition of *z-order signature* is as follows.

Definition 4. ***(z-order Signature).*** *Given a grid C_θ, the z-order signature of the spatial dataset D is a sorted integer set consisting of a sequence of cell IDs, i.e., $z(D) = \{c.id_1, \ldots, c.id_{|z(D)|}\}$, where each element $c.id$ indicates that at least one spatial point from D falls within the cell c.*

3.2 Similarity Measures

To handle search scenarios with varying levels of granularity, we employ two types of measures to compute the dataset similarity.

3.2.1 Overlap-based Similarity Measures

Definition 5. ***(Intersecting Area (IA))*** *Given a query dataset Q and a spatial dataset D, the IA between Q and D is the size of the intersecting area of two given datasets' MBR, i.e., $IA(Q, D) = \prod_{i=1}^{2} l(i, Q, D)$, where $l(i, Q, D)$ denotes the intersecting length of two MBRs in i-th dimension [84].*

Definition 6. ***(Grid-Based Overlap (GBO)).*** *Given a query dataset Q and a spatial dataset D, the GBO between Q and D is the*

number of set intersections of two given datasets' z-order signature $z(Q)$ and $z(D)$, i.e., $G(Q, D) = |z(Q) \cap z(D)|$.

3.2.2 ***Point-wise Similarity Measure*** From the above definitions, we can observe that these two similarity measures only work for overlapping datasets. To address this, we introduce a more fine-grained measure, Hausdorff distance [46], which considers the distance between each pair of points for two datasets.

Definition 7. ***(Hausdorff Distance (Haus)).*** *Given a query dataset Q and a spatial dataset D, the Hausdorff distance from Q to D is the greatest of all the distances from any point $p \in Q$ to the closest point $p' \in D$, i.e.,*

$$H(Q, D) = \max_{p \in Q} \min_{p' \in D} ||p, p'||, \tag{2}$$

where $||p, p'||$ denotes the Euclidean distance between p and p'.

3.3 Types of Dataset Search

In what follows, we introduce two types of dataset search based on the query range and three aforementioned similarity measures, to help users find datasets of interest.

Definition 8. ***(Range-based Dataset Search (RangeS)).*** *Given a rectangular range $R = [p_{min}, p_{max}]$, where p_{min} and p_{max} are the bottom left and upper right points to bound the range R, and a spatial data repository $\mathcal{D}$, a range-based dataset search returns all datasets $\mathcal{D}_q \subseteq \mathcal{D}$ such that: $\forall D \in \mathcal{D}_q$, the MBR of D overlaps with R.*

Definition 9. ***(Top-k Exemplar Dataset Search (ExempS)).*** *Given a query dataset Q and a spatial data repository $\mathcal{D}$, a top-k exemplar search returns k datasets from $\mathcal{D}$ that are most similar to Q, i.e., it retrieves $\mathcal{D}_q \subseteq \mathcal{D}$ with k datasets such that: $\forall D \in \mathcal{D}_q$ and $\forall D' \in \mathcal{D} \backslash \mathcal{D}_q$, we have $dist(Q, D) \leq dist(Q, D')$, where $dist$ is any of the distance measures defined in Section 3.2.*

3.4 Types of Data Point Search

After searching related datasets, the goal of a more fine-grained query is to find the data point of interest.

Definition 10. ***(Range-based Point Search (RangeP)).*** *Given a query range R, and a dataset $D \in \mathcal{D}_q$, the range-based point search returns all the points of D inside the range R.*

Definition 11. ***(Nearest Neighbor Point Search (NNP)).*** *Given a query dataset Q, and a dataset $D \in \mathcal{D}_q$, the NNP search aims to find nearest points in D for each point in Q.*

3.5 Problem Formulation

Definition 12. ***(Spatial Data Search Problem).*** *We aim to propose a highly-efficient and scalable data search system that seamlessly integrates dataset and data point search with a unified index and several acceleration strategies, to work with different types of query types and distance measures.*

RoadMap. The rest of this paper is organized as follows. We first introduce the overall system architecture in Section 4. Then, we describe the unified index and how it is constructed in Section 5. Subsequently, we introduce a series of effective acceleration and pruning mechanisms in Section 6. Finally, experimental results are provided in Section 7.

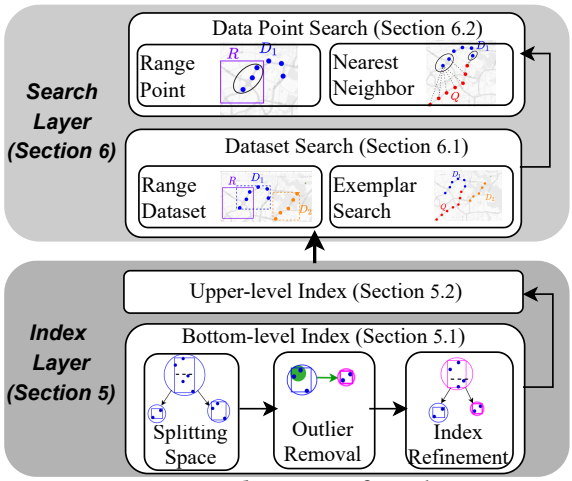

Figure 3: Architecture of Spadas.

4 Spatial Data Search System Framework

Given the problem described in Section 3, we propose a multi-granularity spatial data search system called Spadas. The architecture of Spadas and its components are shown in Fig 3. It consists of two layers that we describe below.

4.1 Index Layer

Existing indexes mainly adopt a single-level index structure that only focuses on dataset-level or data point-level searches. To effectively support a rich set of queries presented in Section 3, we design a novel two-level unified index structure in the index layer, including the upper-level index and bottom-level index, effectively organizing datasets and data points.

Bottom-level Index. The bottom-level index mainly focuses on the spatial distribution of data points within each dataset. For the bottom index, we split the dataset node to create a *dataset index* structure for fine-grained similarity measures and data point searches. Considering that outliers can lead to imbalanced splits and degrade query performance, we first design *parameter-free outlier removal* and *index refinement* techniques to optimize the bottom-level index, which effectively removes outliers and improves the accuracy of similarity computations.

Upper-level Index. The upper-level index is designed to partition and organize datasets at a higher level. Specifically, to avoid scanning all datasets and achieve a fast dataset search for a given query, we pre-organize the indexes of all datasets using a fast space-splitting indexing mechanism, such as the ball-tree [48]. This allows us to construct an upper-level index, referred to as the *data repository index*, which bounds all the dataset nodes. The index construction details are elaborated in Section 5.

4.2 Search Layer

In the search layer, we support both coarse-grained dataset search and fine-grained data point search based on different queries and distance metrics. For dataset search, users have the option to specify a query region R to identify all datasets overlapping with R. Alternatively, they can input a query dataset Q to search for the top-k datasets that have the minimum distance to Q. After searching the datasets of interest, users can select one dataset for more

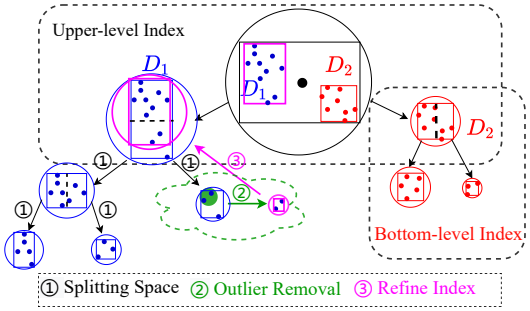

Figure 4: An overview of our unified index.

fine-grained data point searches. These queries can help users find data points of interest to enrich the given query dataset. To accelerate all search operations, we design a set of pruning mechanisms based on the unified index at the search layer. In the following, we describe the basic intuition of pruning mechanisms.

Pruning Mechanisms. Based on building a two-level index, we design a set of unified pruning mechanisms to accelerate multiple types of search operations without constructing additional indexes. Specifically, when the query region R or the query dataset Q arrives, we traverse the index from the upper-level index to the bottom-level index in a depth-first manner. Then, we take the branch-and-bound strategy to batch prune out those nodes that cannot satisfy the query request, significantly speeding up the dataset search. The detailed pruning mechanisms are elaborated in Section 6.

5 Optimization of Index Layer

This section provides a detailed introduction to the index layer. Specifically, we design a unified index based on the whole spatial data repository (see Def. 3), which includes a bottom-level index (see Section 5.1) and an upper-level index (see Section 5.2). Figure 4 presents an overview of our indexing framework. The index is built over a tree structure with nodes bounded by balls and boxes, and we store such bounding information to support multiple types of queries on spatial data. Algorithm 1 shows the details about the implementation of index construction, which will be further explained in the following sections. In the subsequent subsections, we will introduce how the bottom-level (Section 5.1) and upper-level index (Section 5.2) are constructed in detail.

5.1 Bottom Level: Index of Each Single Dataset

As shown in Figure 4, the bottom-level index is built for each dataset, primarily storing the distribution information of data points within each spatial dataset. Since outlier points in the dataset affected the accuracy of spatial dataset search, we also propose a parameter-free outlier removal technology in constructing the bottom-level index, which could effectively remove outliers in the dataset. In the upcoming sections, we will start by introducing the index nodes with multiple attributes to form the bottom-level index. Subsequently, we will introduce the process of bottom-level index building in detail. To construct the bottom-level index, we first transform each spatial dataset D into a dataset root node N_D.

Dataset Root Node. Given a spatial dataset D, a dataset root node N_D corresponding to the dataset D is denoted as a tuple $(id, z, L_p, o, r, N_l, N_r, b^{\uparrow}, b^{\downarrow})$, where id denotes the identifier of the dataset D, z denotes the z-order signature (defined in Def. 4) of D,

Algorithm 1: ConstuctIndex($\mathcal{D}, f, d$)

Input: $\mathcal{D}$: spatial data repository, f: leaf node capacity, d: dimension of spatial point
Output: N_{root}: the root node of unified index

List of dataset root nodes $L \leftarrow \emptyset$;
Initial a sorted list $\phi \leftarrow \emptyset$; ▷ recording leaf nodes' radii
foreach $D_i \in \mathcal{D}$ **do**
  $N_{D_i} \leftarrow$SplitSpace(D_i,f,d,ϕ); ▷ bottom-level index
  $L.add(N_{D_i})$;
OutlierRemoval(L, ϕ); ▷ parameter-free outlier removal
$N_{root} \leftarrow$ SplitSpace($L, f, d, \emptyset$);▷ upper-level index
return N_{root};

Function SplitSpace(S, f, d, ϕ):
  Input: S: data point set or dataset node set, f: capacity, d: dimension, ϕ: sorted list of leaf node radius
  Output: N_s: dataset index node that bounds set S
  $max_width \leftarrow -\infty, d_{split} \leftarrow 0$;
  $leftChildList \leftarrow \emptyset, rightChildList \leftarrow \emptyset$;
  $N_s \leftarrow$ Generate a index node according to set S;
  if *S is a set of data points and $|S| \leq f$* **then**
    $\phi.add(N_s.r)$;
    return N_s;
  if *S is a set of dataset nodes and $|S| \leq f$* **then**
    return N_s;
  for $i \leftarrow 1 : d$ **do**
    if $N_s.b^{\uparrow}[i] - N_s.b^{\downarrow}[i] > max_width$ **then**
      $d_{split} \leftarrow i$;
      $max_width \leftarrow N_s.b^{\uparrow}[i] - N_s.b^{\downarrow}[i]$;
  foreach *each object s in S* **do**
    if *s is a dataset node* **then**
      $temp \leftarrow s.o[d_{split}]$;
    else
      $temp \leftarrow s[d_{split}]$; ▷ s is a data point
    if $temp > N_s.b^{\downarrow}[d_{split}] + \frac{max_width}{2}$ **then**
      $leftChildList.add(s)$;
    else
      $rightChildList.add(s)$;
  $N_s.N_l \leftarrow$ SplitSpace($leftChildList, f, d, \phi$);
  $N_s.N_r \leftarrow$ SplitSpace($rightChildList, f, d, \phi$);
  return N_s;

Function OutlierRemoval(L, ϕ):
  Input: L: list of dataset root nodes, ϕ: sorted list of leaf node radius
  $g' \leftarrow 0, i \leftarrow 1, pos \leftarrow 1$;
  foreach *i-th element in ϕ* **do**
    $g_i \leftarrow$ Equation 3, $i \leftarrow i + 1$;
    if $g_i > g'$ **then**
      $g' \leftarrow g_i, pos \leftarrow i - 1$;
  $r' \leftarrow \phi[pos - 1]$;
  foreach *leaf root node N_{D_i} in L* **do**
    RefineBottomUp(N_{D_i}, r');

Function RefineBottomUp(N, r'):
  Input: N: dataset index node, r': radius threshold
  if *N is a leaf node* **then**
    if $N.r > r'$ **then**
      foreach *point p in N* **do**
        if $||N.o, p|| > r'$ **then**
          $N.L_p.remove(p)$;
    N.update($o, r, b^{\uparrow}, b^{\downarrow}$);
  else
    RefineBottomUp(N_r, r');
    RefineBottomUp(N_l, r');

L_p is a list of nodes contained in dataset D, o is the center point, r is the radius, N_l and N_r are the left and right child nodes, and $b^{\downarrow}$ and $b^{\uparrow}$ are the bottom left and upper right corners of the dataset D's MBR (defined in Def. 2).

We compute the center point o of N_D by averaging the coordinates of all the points in L_p, and choose the farthest distance from o to any point in L_p as the radius r. N_l and N_r are the two child nodes generated during the construction of the index tree. In the bottom-level index, except the root node, internal nodes and leaf nodes are collectively referred to as the dataset index node, which is introduced as follows.

Dataset Index Node. A dataset index node N in the bottom-level index is denoted as a tuple $(L_p, o, r, N_l, N_r, b^{\uparrow}, b^{\downarrow})$, where the meanings of the symbols in this tuple are consistent with those used in the dataset root node.

Algorithm 1 presents the detailed procedure for constructing the bottom-level index, which is comprised of three steps: splitting space, parameter-free outlier removal, and bottom-up index refinement. Firstly, for each dataset $D \in \mathcal{D}$, we perform the function `SplitSpace` of Algorithm 1 for each dataset (see Lines 11 to 34).

Step1: Splitting Space. Given a spatial dataset D, we start by transforming the dataset into its corresponding root node (see Line 13). Then, we compute the width of the root node in each dimension and select the d_{split}-th dimension with the maximum width to split the root node into two child nodes (see Lines 29 to 31). Then, we continue to build the sub-tree for each of the two child nodes (see Lines 32 to 33). On the contrary, if the size of data points in the dataset does not exceed the leaf node capacity f, the process of splitting space terminates (see Lines 14 to 16).

Step2: Parameter-free Outlier Removal. Most existing methods utilize the dataset index to remove outliers that have a limited number of neighbors within a threshold distance, and reconstruct the index [15, 32, 49, 60, 61]. Their common drawback is the high complexity and the requirement of specifying parameters such as the number of neighbors and threshold distance. Thus, we design a parameter-free mechanism to efficiently remove outliers in spatial datasets, utilizing the distribution of leaf node sizes in the dataset index (see Function `OutlierRemoval` of Algorithm 1).

We observe in Figure 5 that there is only a small number of leaf nodes with a large radius in the index built for the two data repositories considered (see Section 7 for more details). We infer that the leaf nodes with large radius may contain outliers because outliers are normally far from other points in the datasets. Hence, a key question here is how to determine an appropriate radius to distinguish between nodes with or without outliers.

The main idea of our method is illustrated in Figure 6. Firstly, it computes the radii of all leaf nodes and sorts them in an array ϕ. It then extends *the Kneedle algorithm* [6, 56] to automatically select an appropriate threshold r' based on the sorted array ϕ. Specifically, it computes a gap (g_i) for a radius $\phi[i]$ as (see Lines 37 to 38):

$$g_i = \phi[0] - i \times \frac{\phi[0] - \phi[|\phi| - 1]}{|\phi|} - \phi[i], i \in \{1, |\phi - 1|\}. \quad (3)$$

Geometrically, the gap g_i for a radius $\phi[i]$ computes the distance between the point $(i, \phi[i])$ and its projection on the segment connecting the first point $(0, \phi[0])$ and the last point $(|\phi|-1, \phi[|\phi|-1])$,

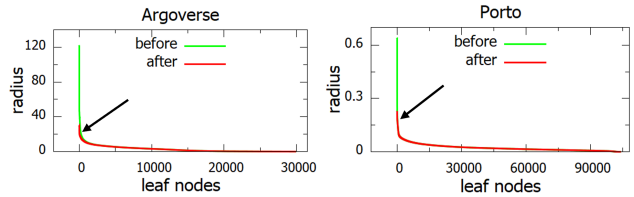

Figure 5: The distributions of radii of leaf nodes before and after outlier removal on two data repositories.

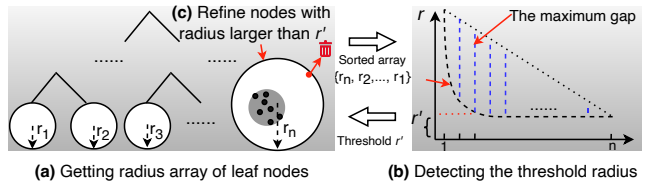

Figure 6: An illustration of the proposed parameter-free outlier removal method based on the Kneedle algorithm.

as shown in Figure 6(b). The radius with the largest gap is selected as the threshold r' (see Lines 39 to 41), as it is the turning point where most leaf nodes start to have a similar radius. Thus, leaf nodes with a radius greater than r' are refined by removing potential outliers.

Step3: Bottom-Up Index Refinement. With the radius threshold r', we traverse up from all leaf nodes to refine the dataset index until reaching the dataset root node in a dataset index. Specifically, for each leaf node, we remove all the points p' that have a distance to the pivot point p larger than r' (see Lines 45 to 50), then refine the node and its upper-level nodes recursively in Function `RefineBottomUp` (see Lines 52 to 53).

5.2 Upper Level: Data Repository Index

After constructing the bottom-level index, we further create an upper-level index in a similar top-bottom way to organize close nodes together. In the following, we will first introduce the index node in the upper-level index, followed by a detailed explanation of how the upper-level index is constructed.

Data Repository Index Node. A data repository index node N is denoted as a tuple $(o, r, N_l, N_r, b^{\uparrow}, b^{\downarrow}, z, \delta)$, where δ indicates whether N is a leaf node, z is the union of signatures of all its child nodes (i.e., $N.z = \bigcup_{N' \in N_l \cup N_r} N'.z$), and the meanings of other symbols in the tuple are the same as in the dataset root node.

As shown in Figure 4, the upper-level index is constructed in a similar way to the bottom-level index (see Line 7). Given a list of dataset root nodes L, we first initialize a dataset repository index node for the list L, and choose the widest d_{split}-th dimension to split the L into two child lists based on their position in relation to the split line of parent node's MBR. Then, we create the dataset repository index node for each of the two child lists and continue to build the sub-tree, until the size of the child list satisfies the leaf node capacity f (see Lines 17 to 18).

Time Complexity. Additionally, we provide a theoretical analysis of the time complexity for constructing the unified index, which is $O(mn \log(n))$, where m and n represent the number of data points in the dataset and the number of datasets in the data repository, respectively. The detailed analysis is provided in Appendix 9.2.

Novelty of Unified Index. In the process of index construction, previous indexes are designed for either spatial datasets or data points, which cannot support multiple types of searches. Thus, we design a two-level index structure, effectively organizing both datasets and data points, and can support spatial data search of different granularity at the same time. In addition, the existing indexes do not consider the influence of outliers in spatial datasets. Thus, we innovatively design outlier removal and index refinement technologies in index construction, to mitigate the influence of outliers on the accuracy of similarity measures between datasets.

6 Optimization of Search Layer

Based on the unified index constructed in the previous section, we propose effective pruning mechanisms to solve the data search problem defined in Section 3.5.

6.1 Accelerating Dataset Search

In this subsection, we describe the dataset search algorithm applied to range-based dataset search and top-k exemplar dataset search defined in Section 3.3. Algorithm 2 shows the details of the implementation of the algorithm.

6.1.1 Accelerating Range-based Dataset Search Firstly, we introduce the accelerating strategy over range-based dataset search, as defined in Def. 8, which only involves traversing the upper-level index to find datasets that overlap with the query region R. Specifically, we start from the root node of the upper-level index and traverse all its child nodes that intersect with R. Subsequently, we can directly prune the non-intersecting child nodes. For the intersecting child nodes, we iteratively traverse their child nodes if they are not leaf nodes; otherwise, we add their corresponding dataset IDs to the result list (see Lines 2 to 4). Finally, we return the result list that covers all datasets that overlap with R.

6.1.2 Accelerating Top-k Exemplar Dataset Search To accelerate the top-k exemplar dataset search defined in Def. 9, which supports two types of similarity queries: overlap-based queries (IA defined in Def. 5 and GBO defined in Def. 6) and point-wise distance query (Haus defined in Def. 7), we propose a series of acceleration strategies. Compared to the other two measures, the Hausdorff distance has a quadratic computational complexity in terms of the number of points in the datasets. Thus, we propose a fast bound estimation technique to speed up the computation of the Hausdorff distance. In addition, to get the query results faster, users are often satisfied with approximate answers, especially if precision guarantees accompany these answers. Thus, we also propose a fast and efficient approximate Hausdorff distance computation with a theoretical error guarantee to balance efficiency and effectiveness.

(1) Overlap-based Queries. In overlap-based queries, we have a ranking list that holds k datasets with the maximum overlap. Given a data repository node, we can prune it if (i) there is no overlap or (ii) the overlap-based distance (see Line 18) is bigger than the k-th result. Taking the top-k GBO search as an example, if a dataset repository node N has fewer intersected grids with the query than the current k-th result, we can directly prune N and all sub-trees of N, which greatly reduces the number of candidate datasets.

Algorithm 2: DatasetSearch(Q or R, $\mathcal{D}$, N, k)

Input: Q or R: query dataset or range, $\mathcal{D}$: data repository, N: a node in the index, k: number of results
Output: $\mathcal{R}esult$: result list

```
1  Result ← ∅;
2  if N is a dataset root node then
3      if Range-based query then
4          Add N.id and update Result;
5      else
6          if Haus then
7              dis ← HausCompute(Q, N);
8          else
9              if IA || GBO then
10                 dis ← Compute dis between Q and N;
11         if dis < Result[k] then
12             Add N.id and rank Result increasingly by dis;
13 else
14     foreach child node N_c ∈ N.N_l ∪ N.N_r do
15         if Range-based query then
16             Result.add(DatasetSearch(R, D, N_c, k));
17         else
18             dis ← compute dis between Q and N_c;
19             if dis < Result[k] then
20                 Result.add(DatasetSearch(Q, D, N_c, k));
21 return Result;
```

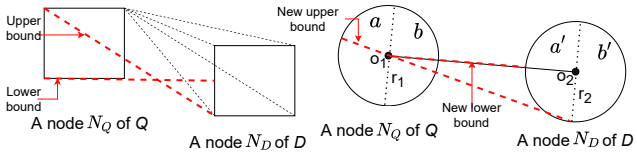

(a) Bounds based on bounding rectangles (b) Bounds based on bounding balls

Figure 7: The distance bounds between two nodes using bounding boxes (left) and bounding balls (right).

(2) Point-wise Distance Query. As a point-wise distance measure, the computation time of Hausdorff increases dramatically with the number of points in the dataset since it has a quadratic time complexity. To accelerate Hausdorff's computation, we propose a *fast bound estimation* technique to efficiently estimate the lower and upper bounds of Hausdorff distance, as detailed below.

Fast Bound Estimation. We propose an efficient algorithm based on bounding balls of nodes to estimate the lower and upper bounds of the Hausdorff distance between nodes, which is not affected by the dimensions and only needs a single distance computation between center points. In contrast to the R-tree based incremental approach [46], which requires enumerating all pairs of corners of nodes' bounding boxes (as illustrated by the four black dotted lines in Figure 7(a)), our method avoids quartic Euclidean distance computations [46] and only requires a single computation.

Next, we take Figure 7(b) as an example to elaborate on the lower and upper bounds of the Hausdorff we propose. When we construct an index node to bound all the points, for any diameter (see the two black dotted lines in Figure 7(b)) that divides the ball into two half-balls, each part should have at least one point. Otherwise, the ball should be refined to a ball with a smaller radius. We assume the two half balls are a and b of Q, a' and b' of D, and b and a' are two close half-balls. Since the Hausdorff distance is the greatest

Algorithm 3: HausCompute(Q, N_D)

Input: Q: query dataset, N_D: dataset root node
Output: UB: Hausdorff distance between Q and D

1 $N_Q \leftarrow$ create a dataset root node of Q;
2 **if** ***Haus*** **then**
3 $\quad PQ^{\uparrow} \leftarrow$ CreateAscendingPQ(), $PQ^{\uparrow}.Insert(N_D, 0)$;
4 $\quad PQ^{\downarrow} \leftarrow$ CreateDescendingPQ(), $PQ^{\downarrow}.Insert(N_Q, \infty, PQ^{\uparrow})$;
5 **while** $PQ^{\downarrow}.nonEmpty()$ **do**
6 $\quad [N_Q, UB, PQ^{\uparrow}] \leftarrow PQ^{\downarrow}.Dequeue()$;
7 $\quad [N_D, LB] \leftarrow PQ^{\uparrow}.Head(), terminate \leftarrow false$;
8 $\quad$ **if** ***Appro*** **then**
9 $\quad\quad$ **if** $N_D.r < \epsilon$ *and* $N_Q.r < \epsilon$ **then**
10 $\quad\quad\quad terminate \leftarrow true$;
11 $\quad$ **if** *terminate* **then**
12 $\quad\quad$ **return** UB;
13 $\quad$ **else**
14 $\quad\quad$ **if** $N_D.r > N_Q.r$ **then**
15 $\quad\quad\quad$ TraversalDIndex($N_Q, PQ^{\uparrow}, PQ^{\downarrow}$);
16 $\quad\quad$ **else**
17 $\quad\quad\quad$ TraversalQIndex($N_D, PQ^{\uparrow}, PQ^{\downarrow}, UB$);
18

Function TraversalQIndex($N_Q, PQ^{\uparrow}, PQ^{\downarrow}$):
$\quad$ **Input:** N_Q: query node, $PQ^{\uparrow}$: main queue, $PQ^{\downarrow}$: second queue
19 $\quad$ **foreach** *child* N_C *in* N_Q **do**
20 $\quad\quad CPQ^{\uparrow} \leftarrow CreateAscendingOrderPQ(), minUB \leftarrow \infty$;
21 $\quad\quad$ **foreach** *child node* $N_C \in PQ^{\uparrow}$ **do**
22 $\quad\quad\quad CPQ^{\uparrow}.insert(N_C, \text{LowerBound}(N_C, N_D))$;
23 $\quad\quad\quad minUB \leftarrow \min(minUB, \text{UpperBound}(N_C, N_D))$;
24 $\quad\quad PQ^{\downarrow}.Insert(N_C, minUB, CPQ^{\uparrow})$;
25

Function TraversalDIndex($N_D, PQ^{\uparrow}, PQ^{\downarrow}, UB$):
$\quad$ **Input:** N_D: dataset node, $PQ^{\uparrow}$: main queue, $PQ^{\downarrow}$: second queue, UB: the upper bound
26 $\quad [N_D, LB] \leftarrow PQ^{\uparrow}.Dequene(), minUB \leftarrow UB$;
27 $\quad$ **foreach** *child* $N_C \in N_D$ **do**
28 $\quad\quad CPQ^{\uparrow}.insert(N_C, \text{LowerBound}(N_Q, N_C))$;
29 $\quad\quad minUB \leftarrow \min(minUB, \text{UpperBound}(N_Q, N_C))$;
30 $\quad PQ^{\downarrow}.Insert(N_Q, minUB, PQ^{\uparrow})$;

of all distances from any point $p \in Q$ to the closest point $p' \in D$, the closest point pair (p, p') with the greatest distance in the Hausdorff distance computation from Q to D should be in a and a'. We can easily get that $\forall p \in a, p' \in a'$, $||p, p'|| \geq ||o_1, o_2|| - r_2$, and $||p, p'|| \leq \sqrt{||o_1, o_2||^2 + r_2^2} + r_1$ according the triangle inequality. Still taking Figure 7(b) as an example, the lower bound should be the distance from o_1 to the closest point in the node N_D. The upper bound of the nearest neighbor will be the distance from the most left of Q to the farthest in the left part of D. Hence, the Hausdorff distance $H(Q, D)$ between Q and D can be bounded in the range:

$$\left[\max(||o_1, o_2|| - r_2, 0), \sqrt{||o_1, o_2||^2 + r_2^2} + r_1\right]. \tag{4}$$

Exact Hausdorff. The above bounds can also be directly used in the fast pairwise Hausdorff distance computation. The main idea is to rank candidates based on two priority queues. Algorithm 3 shows how to prune distance computations based on bounds and achieve early termination without computing the full distance between all pairs of points from Q and D. Similar to the incremental traversal (Please refer to Algorithm 4 in [46])[2], since the goal of Hausdorff is to calculate the maximum nearest neighbor distance, we first create a priority queue in descending order, ranking the distance from the point to their nearest neighbors. Then to compute the minimum distances to the nearest neighbors for points in Q, we further create an ascending priority queue to traverse the dataset from close to far. Subsequently, we traverse the index of Q and D from the root nodes, estimate the bounds between the polled pair of nodes, and conduct pruning. The whole algorithm terminates when the first pair of points are polled from the main priority queue. For convenience, we refer to this method as "**ExactAppro**" in Section 7.

Approximate Hausdorff. Computing the exact Hausdorff distance can be time-consuming by going to the lowest point level of the dataset index. Instead, we can calculate an *error-bounded Hausdorff distance* in a more efficient way based on the unified index. In the exact distance computation, we terminate until a pair of points show up from the queue. To avoid such intensive distance computations, we set a rule that once a pair of "small" nodes have a radius smaller than a given threshold ϵ (see Line 8), we compute their Euclidean distance between their center points. Then we return the distance $||o_1, o_2||$ as the approximate distance, and do not enqueue their child nodes or points anymore. For convenience, we refer to this method as "**ApproHaus**" in Section 7. Next, we prove that the **ApproHaus** method in Lemma 1 achieves a guaranteed precision of 2ϵ, where ϵ is the error threshold defined by the user.

Lemma 1. *Given a threshold ϵ, the approximate algorithm guarantees an error of 2ϵ for the Hausdorff distance.*

Proof. Based on the bound in Inequation 4, we can get the upper bound distance and lower bound distance. When two nodes' radii are given, we can estimate the error bound based on the gap between their upper bounds and lower bounds:

$$\sqrt{||o_1, o_2||^2 + r_2^2} + r_1 - ||o_1, o_2|| \leq r_1 + r_2 < 2\epsilon, \tag{5}$$

where we apply the triangle inequality:

$$\sqrt{||o_1, o_2||^2 + r_2^2} - ||o_1, o_2|| \leq r_2. \tag{6}$$

For the lower bound, we can prove that:

$$\max(||o_1, o_2|| - r_2, 0) - ||o_1, o_2|| = -r_2 \geq -\epsilon, \tag{7}$$

which holds for both $||o_1, o_2|| \geq r_2$ and $||o_1, o_2|| \leq r_2$. Then, we proved that the error is bounded by 2ϵ. □

To select a proper ϵ, we can choose the cell size as the error threshold ϵ according to the MBR range as follows:

$$\epsilon = \frac{b^{\uparrow}[0] - b^{\downarrow}[0]}{2^{\theta}}. \tag{8}$$

6.2 Accelerating Data Point Search

6.2.1 Range-based Point Search Given a query range R and a dataset D from the query result $\mathcal{D}_q$, the range-based point search defined in Def. 10 aims to identify all points in D that fall within the specified range. To expedite the range-based point search process, we employ a depth-first traversal approach starting from the root node N_D of the dataset. During the traversal, we can prune the dataset

[2]Readers can refer to Algorithm 4 of [46] for more details. Here, we will skip them as the estimation of the bounds is our main focus.

Table 1: Summary of six spatial data repositories.

Data repository	# of datasets	# of dimensions	Size (GB)
MultiOpen	10,714	2	4.39
T-drive	250,606	2	0.79
Argoverse	280,000	3	17.87
ShapeNet	32,135	3	2.04
Chicago	283,375	11	1.99
Porto	1,400,000	2	1.45

index node N if there is no overlap with the query rectangle R, i.e., $R \cap N.b = \emptyset$. Conversely, if there is an intersection, we proceed to evaluate the relationship between the node N and R. When the query range R entirely encompasses the node N, all data points beneath that node are added to the result list. For the intersecting node with R, we iteratively traverse their children until reaching leaf nodes. At each leaf node, we identify the specific points that fall within the range R and append them to the result set.

6.2.2 Nearest Neighbor Point Search In nearest neighbor point search defined in Def. 11, for each point in the query set Q, we select a dataset D from the query result $\mathcal{D}_q$ and find the nearest neighbor point within D. A naive way to accelerate this is by using the nearest neighbor search with the dataset index, which is similar to the Hausdorff distance computation. Since the Hausdorff queries have conducted the pruning of point pairs that are far, we can reuse the queues $PQ^{\uparrow}$ and $PQ^{\downarrow}$ during pairwise Hausdorff matching and further process based on the dataset index to accelerate the nearest neighbor point search. With the cached priority queue in our Algorithm 3, we keep en-queuing the node pair until the queue is empty, then every query point will find its nearest neighbor.

Novelty of Acceleration Strategies. According to the links between these technological developments, we can see that the proposed acceleration strategies based on our two-level unified index can solve multiple types of search problems at the same time compared to previous methods, which can only solve a single search problem [14, 35, 40]. In addition, we theoretically derive Hausdorff's upper and lower bounds using the triangle inequality, and we explore the approximate Hausdorff value in depth with a guaranteed theoretical error.

7 Experiments

We conduct experiments on six real-world dataset repositories to demonstrate the effectiveness and efficiency of Spadas. In Section 7.1, we introduce the experimental setups. Then, we present the performance of our proposed unified index in Section 7.2. Next, we present the experimental results that vary with several key parameters to demonstrate the effectiveness and efficiency of the dataset search and data point search in Sections 7.3 and 7.4, followed by our case study in Section 7.5.

7.1 Settings

Datasets. We conduct experiments on six representative spatial dataset repositories, each of which is downloaded from open-source spatial data portals. Table 1 presents the scale and dimension of each data repository. Figure 8 shows the distributions of the number of points in each data repository.

Table 2: Parameter settings.

Parameter	Setting
k: number of results	{<u>10</u>, 20, 30, 40, 50}
m: number of datasets	$\{10^{-4}, 10^{-3}, 10^{-2}, 10^{-1}, \underline{1}\}\times\lvert\mathcal{D}\rvert$
θ: resolution	{3, 4, <u>5</u>, 6, 7}
R: query range	$\{1, 2, \underline{3}, 4, 5\}\times\epsilon$
s: # of combined datasets	$\{\underline{1}, 10, 10^2, 10^3, 10^4\}$
f: leaf node capacity	{<u>10</u>, 20, 30, 40, 50}
d: dimension	{<u>2</u>, 4, 6, 8}

- **MultiOpen** dataset, a real-world spatial data repository comprising datasets collected from three different open-source platforms: Points of Interests (POIs) of Baidu Maps Open Platform [7], BTAA Geoportal [2] and NYU Spatial Data Repository [4].
- **T-drive** dataset [76] contains a collection of real-world trajectory datasets generated by over 33,000 taxis in Beijing;
- **Argoverse** self-driving datasets [21] which record five-second driving scenarios with thousands of points;
- **ShapeNet** [20], large-scale datasets of shapes represented by 3D computer-aided design (CAD) models of objects;
- **Chicago** taxi trips [3] dataset, which has 194,992,061 trips in total. As all the trips are quantized every 15 minutes, we split the whole dataset every 15 minutes to create a set of sub-datasets, and there are 283,375 datasets in total;
- **Porto** dataset [5] transformed from 400+ taxis' trajectories in the city of Porto for one year.

Implementation. We implement Spadas using Java 1.8 and run all our experiments on a 2x Intel Xeon Platinum 8268 24C 205W 2.9GHz Processor with 32G memory. Our code and guidelines for reproducibility can be accessed on the GitHub [10]. We also have an online demonstration system [11] on the Argoverse data repository, which supports the dataset and data point search proposed in this paper, and our proposed top-k EMD search [70] is also available.

Query Generation. We randomly extract 100 datasets from each data repository as the query datasets to search the rest, and the final running time is logged on average from these 100 query datasets. For the range-based query, we get the root node of each query dataset and infer the center point o, and we increase the number of cells to simulate the increasing range R around o to observe their effects on the performance.

Parameter Settings. The settings of parameters are summarized in Table 2 where the default settings are underlined. Below is the description of each parameter:

- k: It specifies the number of results in the exemplar search.
- m: It specifies the scale of the dataset in each data repository used to verify the scalability of our system.
- θ: It determines the size of cells in the grid.
- R: It determines the range of query rectangular, where ϵ is the value obtained when the resolution θ is the default value 5 according to the Equation 8 in Section 6.1.2.
- s: It determines the scale of the query dataset in the nearest neighbor point (NNP) search (e.g., 10 means combining the points from the 10 query datasets into a larger dataset), which can be used to verify the scalability of the NNP.
- f: It specifies the capacity of the leaf node, which is mainly used to determine when to terminate the index construction.

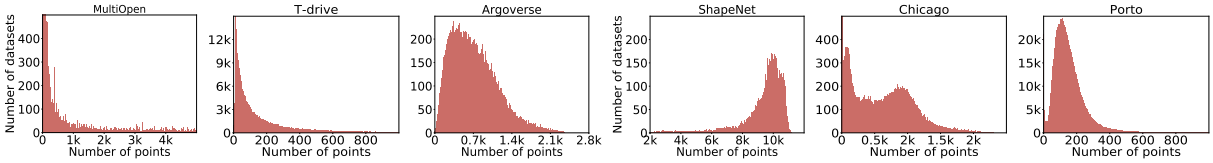

Figure 8: Dataset scale distributions in six data repositories.

Methods for Comparison. We compare our proposed Spadas system against the following baselines.

- RangeS (Def. 8): our range-based dataset search supported by the Spadas system.
- IA (Def. 5): our top-k exemplar dataset search based on the intersecting area supported by the Spadas system.
- GBO (Def. 6): our top-k exemplar dataset search based on the grid overlap supported by the Spadas system.
- ExactHaus: our top-k exemplar dataset search based on the exact Hausdorff distance with a fast bound estimation technique.
- ApproHaus: our top-k exemplar dataset search based on the approximate Hausdorff distance with the error-bounded approximation technique.
- RangeP (Def. 10): our range-based data point search supported by the Spadas system.
- NNP (Def. 11): our nearest neighbor point search supported by the Spadas system.
- ScanGBO [52]: the baseline comparison method needs to scan the candidate datasets to compute the grid-based overlap for each query dataset (see Algorithm 2 in [52]).
- ScanHaus [12]: It designs the lower and upper bounds of Hausdorff by using two point sets' MBR, and combines branch-and-bound to accelerate filter out dissimilar datasets.
- IncHaus [46]: It speeds up the Hausdorff distance computation by incrementally exploring the index of two point sets.
- INNE [13, 80]: the **i**solation-based anomaly detection using **n**earest-**n**eighbor **e**nsembles for outlier removal.
- Origin: The standard method for computing the exact Hausdorff distance without removing any outliers.
- kNN [59]: a nearest neighbor search method using the early break strategy.

7.2 An Overview of spadas

We first show the running time of seven main steps in Spadas system, including the unified index construction (Index), dataset search (RangeS, IA, GBO, ExactHaus), and data point search (RangeP, NNP). As shown in Figure 9, we can observe that unified index construction is the most time-consuming step in most cases. However, the time taken to construct the index is still less than one minute. Moreover, the top-k Hausdorff search is the slowest in dataset search compared with the IA and GBO due to its high complexity, but its running time is still tolerable.

Efficiency of the Unified Index. We compare our unified index with the existing work that constructs an independent index using R-tree [46] in IncHaus. Figure 10 presents the construction cost and the occupied space as the data repository scale m increases. It is evident that our proposed unified index outperforms the state-of-the-art method in terms of both index construction time and space footprint. Specifically, with regard to index construction time, the unified index can achieve at most 36.8% speedup over the index of IncHaus. Additionally, in terms of index space, the unified index is reduced by up to 90% over the IncHaus.

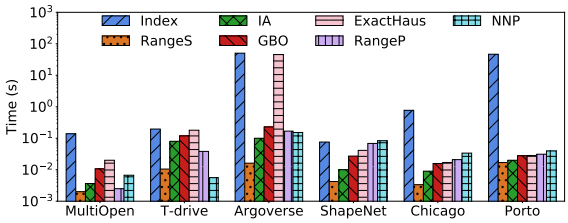

Figure 9: Efficiency in all stages on various data repositories.

7.3 Efficiency of Dataset Search

As the range-based dataset search is very fast (see Figure 9), we mainly test the performance of the top-k exemplar search.

7.3.1 ***Top-k Overlap-based Query*** We vary several key parameters to observe the search performance of overlap-based search.

Effect of Number of Results k. As shown in Figure 11, we increase k to observe the search performance of coarse metrics based on overlaps. We can observe that the IA is the fastest compared to the other two measures, because it only needs to compute the intersection area, while GBO needs to conduct an intersection on integer sets. In addition, GBO consistently outperforms the ScanGBO, which utilizes a sequential scanning approach. Specifically, the GBO can achieve up to at most 53% times speedups over the ScanGBO, which demonstrates the effectiveness of our method.

Effect of Leaf Node Capacity f. We show the results of overlap-based search with the increase of leaf node capacity f. From Figure 12, we can observe that the search time of the three methods does not change significantly with the increase of f, indicating that the leaf node capacity during index construction has little influence on the search efficiency. In addition, we can see that GBO and IA consistently outperform the ScanGBO, indicating that the pruning mechanism based on the unified index is very efficient.

Effect of Grid Resolution θ. Figure 13 shows the performance of GBO as the resolution θ increases. Since increasing θ leads to a higher number of cells spanning the entire space, the cell size is reduced. Thus, this enlarges the z-order signature in each index node, resulting in a degradation of efficiency. Specifically, due to the relatively large size and tight distribution of the Argoverse dataset, increasing θ leads to more pronounced increases in z-order signature, resulting in a greater search time.

7.3.2 ***Top-k Point-wise Query*** We vary several key parameters to test the performance of the exact and approximate Hausdorff.

Effect of Top-k Search. 1) **Exact Hausdorff**. We compare the top-k Hausdorff search performance of our ExactHaus with ScanHaus and IncHaus as k increases. As shown in Figure 14, we can

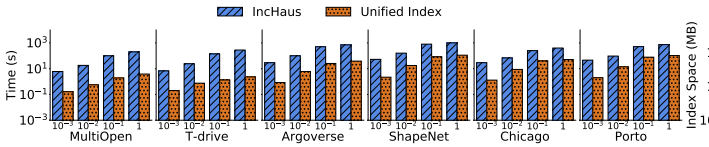

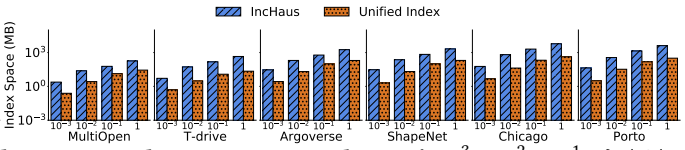

Figure 10: Index's construction time and occupied space with increasing data repository scale $m = \{10^{-3}, 10^{-2}, 10^{-1}, 1\} \times |\mathcal{D}|$.

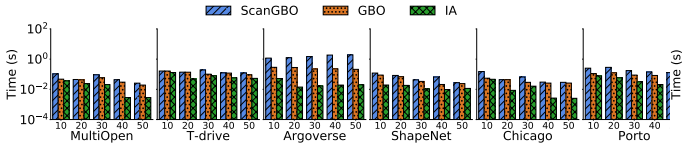

Figure 11: Top-k overlap-based queries as k increases.

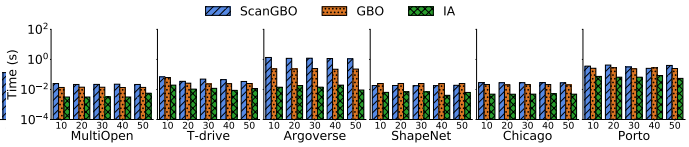

Figure 12: Top-k overlap-based queries as f increases.

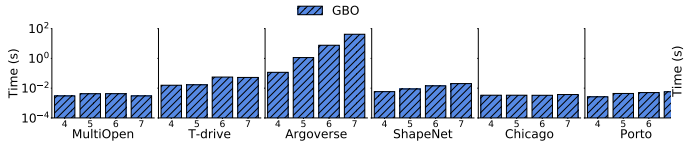

Figure 13: Grid resolution θ's effects on top-k GBO query.

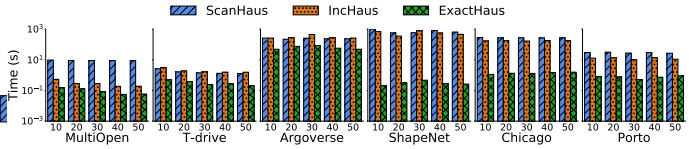

Figure 14: Top-k exact Hausdorff search with increasing k.

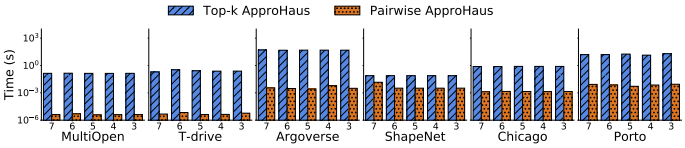

Figure 15: Top-k approximate Hausdorff search with increasing threshold ϵ (i.e., decreasing resolution θ in x-axis).

observe that our ExactHaus based on the unified pruning mechanism drastically improves the performance of top-k Hausdorff search, achieving up to at most three orders of magnitude speed improvements against the ScanHaus and IncHaus. This proves that our fast bound estimation technology is effective.

2) **Approximate Hausdorff**. The approximate Hausdorff is further evaluated by decreasing the error threshold ϵ. Since the error threshold increases as the resolution decreases, we present the experimental results of our proposed ApproHaus in pairwise Hausdorff computation (i.e., computing the Hausdorff distance between two spatial datasets) and top-k Hausdorff search, as the resolution decreases, in Figure 15. We observe that the runtime of pairwise ApproHaus computation degrades slightly with the increase of the error threshold. This is because in order to achieve a smaller error, the algorithm needs to scan more child nodes in the dataset index for approximate Hausdorff computation and terminate later.

Furthermore, as illustrated in Figure 16, we compare the effectiveness and efficiency of top-k GBO and Haus search in two modes: ApproHaus and ExactHaus. We use the top-k search results of ExactHaus as the ground truth (with a constant accuracy of 1 in Figure 16), and the accuracy of ApproHaus is defined as the number of identical datasets between its top-k results and the top-k results of ExactHaus divided by k. The experimental results show that although GBO is faster than the two Hausdorff searches, the accuracy is much lower (less than 80%). In contrast, our ApproHaus algorithm can achieve up to at most 81.6% times speedups over ExactHaus on various data repositories and maintain high accuracy (up to 90%). This proves that our proposed error-bounded approximation technology is effective.

Effect of Outlier Removal. Figure 17 shows the experimental results of top-k Hausdorff search under three conditions: without using outlier removal (Origin), using our ExactHaus, and utilizing the SOTA INNE [13, 80] for outlier removal. The results from INNE are set as the ground truth. Also, we compare the execution time of these two outlier removal algorithms. The results demonstrate that our outlier removal technique can effectively remove outliers in the dataset by detecting leaf nodes with excessively large radii, thereby enhancing the accuracy of the search (up to 90%). Moreover, our algorithm exhibits significantly faster performance, surpassing INNE by five orders of magnitude, due to the substantial reduction in data points achieved by detecting kneedle points.

Effect of Node Capacity f. Figure 18 shows the runtime of the three index-based methods when computing the Hausdorff distance between a pair of datasets. We observe that as the f increases, the execution time of the pairwise Hausdorff gradually increases. This is because larger leaf nodes imply that more data points need to be scanned one by one, which affects the performance. Figure 19 shows that as the capacity of leaf nodes f increases, the running time of the three methods does not change much, indicating that the impact of node capacity on the top-k queries is minimal. This is because more time is spent on pruning, sorting, and computing bounds, rather than scanning the data points within the nodes.

Effect of Dimension d. As the Chicago dataset's dimension is the highest, we use it to verify the performance of three representative operations in Figure 20. Firstly, from the left of Figure 20, we can see that the query time of the two overlap-based methods does not change much with the increase of dimension, and IA is much faster than GBO. The right of Figure 20 shows the search time of the top-k Hausdorff. The experimental result shows that with the increase of d, the running time of the ScanHaus and IncHaus increases, while the times of the ExactHaus do not change significantly. This indicates that dimension significantly affects the effectiveness of calculating distances between MBRs.

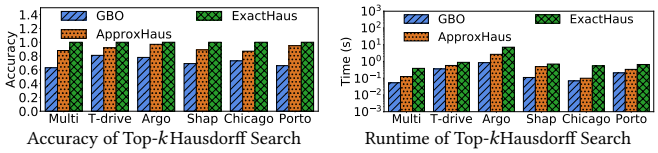

Figure 16: Accuracy and runtime of three exemplar searches.

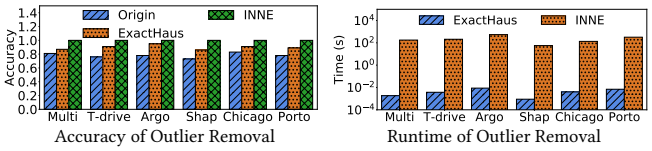

Figure 17: Accuracy and runtime of top-k Hausdorff search.

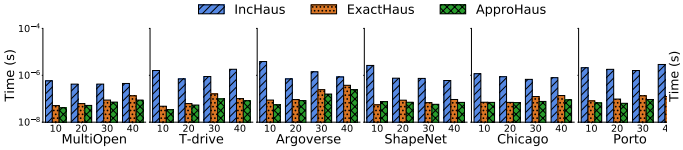

Figure 18: Capacity's effects on pairwise Hausdorff search.

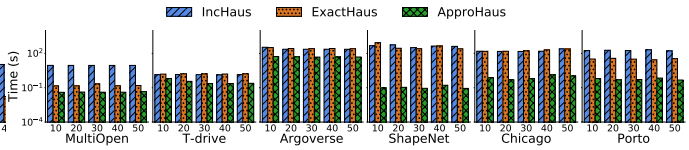

Figure 19: Index capacity's effects on top-k Hausdorff search.

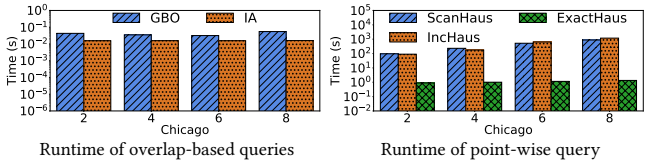

Figure 20: Spatial dimension d's effect on the Chicago dataset.

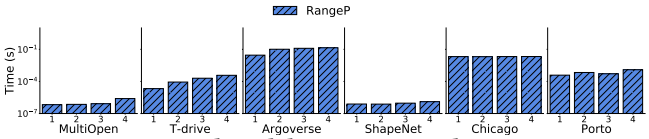

Figure 21: Range-based data point search as R increases.

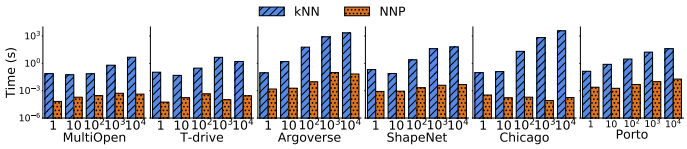

Figure 22: Nearest neighbor point search as s increases.

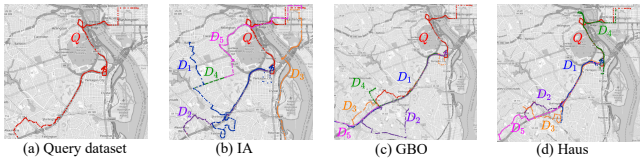

Figure 23: Case study on trajectory datasets.

7.4 Efficiency of Data Point Search

Range-based Point Search. Figure 21 shows the performance of searching all the points located inside a range. We can observe a slight increase in running time as the query range R increases. It is because as the query range increases, the number of candidates falling within the query range increases, so it takes more time to check the increasing number of candidates in a dataset.

Nearest Neighbor Point Search. We mainly compare our NNP search operation presented in Section 6.2 against the k-nearest neighbor (kNN) [59] that works similarly to the Hausdorff distance [46]. Figure 22 shows that our method can accelerate the NNP operation significantly, which achieves up to seven orders of magnitude speedup over kNN. This is because the kNN shares a common procedure with NNP to find the nearest points for points in the query datasets, and we can save much time by continuously traversing the unified index.

7.5 Case Study

Fig. 23 shows the visualization of the results that conduct trajectory search and analysis based on the Spadas system developed in this paper. Specifically, we added a transportation dataset collection to Spadas that includes a variety of trajectory datasets from Washington, D.C. An analyst aims to find k trajectory datasets that are closely similar to a given query dataset from the Spadas to perform trajectory analysis tasks, such as trajectory near-duplicate detection [69] and traffic congestion prediction [81, 83].

As shown in Fig. 23(a), the analyst first inputs a query dataset Q from Washington, D.C. into Spadas, aiming to find the top 5 datasets that are similar to Q. The results found based on IA, GBO, and Haus similarity measures are shown in Figures 23(b), (c), and (d). We can see that the result datasets obtained by IA are coarse-grained compared with GBO and Haus. For example, although the intersecting area between the result dataset D_5 and Q is quite large, their data point distributions are not similar. In contrast, the results obtained by Haus and GBO are more similar to the query Q, but Haus offers a more fine-grained similarity. For example, the result D_2 obtained by Haus is more similar to Q in terms of dataset distribution than D_2 obtained by GBO. The analyst can use these retrieved datasets, along with Q, for trajectory data analysis tasks.

8 Conclusions

We presented Spadas, a multi-granularity spatial data search system that seamlessly supports coarse-grained dataset search based on multiple distance metrics and fine-grained data point search. We first designed a unified two-level index, which can effectively organize spatial datasets to support multiple types of search operations, and mitigate the impact of outliers on the accuracy of similarity measures between datasets. Then, we proposed a range of pruning mechanisms, including fast bound estimation, approximation technique with error bound, and pruning in batch techniques, which can efficiently prune irrelevant datasets and data points, thereby significantly reducing the search overhead. Finally, we conducted extensive experiments using six real-world dataset collections and compared the performance of the proposed algorithms with that of related state-of-the-art algorithms. The results corroborated that the proposed system is effective, efficient, and scalable. In future work, we plan to further evaluate the effectiveness of additional distance measures.

References

[1] Auctus Dataset Search. https://auctus.vida-nyu.org/, 2021.
[2] The big ten academic alliance geoportal. https://geo.btaa.org/, 2021.
[3] Chicago Taxi Trips. https://data.cityofchicago.org/Transportation/Taxi-Trips/wrvz-psew, 2021.
[4] Find maps and data through NYU. https://geo.nyu.edu/, 2021.
[5] Taxi Service Trajectory (TST) Prediction Challenge 2015. http://www.geolink.pt/ecmlpkdd2015-challenge/, 2021.
[6] Knee-point detection in Python. https://pypi.org/project/kneed/, 2022.
[7] Baidu Maps Open Platform. https://lbsyun.baidu.com/, 2023.
[8] Chicago Data Portal. https://data.cityofchicago.org/, 2023.
[9] Foursquare. https://foursquare.com/city-guide, 2024.
[10] Github code. https://github.com/tgbnhy/spadas/tree/lyy, 2024.
[11] Our online demonstration system of spatial data search. http://sheng.whu.edu.cn/prototype/spadas/, 2024.
[12] M. D. Adelfio, S. Nutanong, and H. Samet. Similarity Search on a Large Collection of Point Sets. In *SIGSPATIAL*, pages 132–141, 2011.
[13] T. R. Bandaragoda, K. M. Ting, D. Albrecht, F. T. Liu, Y. Zhu, and J. R. Wells. Isolation-based anomaly detection using nearest-neighbor ensembles. *Computational Intelligence*, 34(4):968–998, 2018.
[14] J. L. Bentley. Multidimensional binary search trees used for associative searching. *Commun. ACM*, 18(9):509–517, 1975.
[15] K. Bhaduri, B. L. Matthews, and n. R. Chris Giannella. Algorithms for Speeding up Distance-Based Outlier Detection. In *KDD*, pages 859–867, 2011.
[16] P. Bouros and N. Mamoulis. Spatial joins: What's next? *SIGSPATIAL Special*, 11(1):13–21, 2019.
[17] T. Brinkhoff, H. Kriegel, and B. Seeger. Efficient processing of spatial joins using r-trees. In *SIGMOD*, pages 237–246, 1993.
[18] C. Cao and M. Li. Generating mobility trajectories with retained data utility. In *SIGKDD*, pages 2610–2620, 2021.
[19] S. Castelo, F. Chirigati, R. Rampin, A. Santos, A. Bessa, and J. Freire. Auctus: A Dataset Search Engine for Data Augmentation. *PVLDB*, 14(12):2791 – 2794, 2021.
[20] A. X. Chang, T. A. Funkhouser, L. J. Guibas, P. Hanrahan, Q. Huang, Z. Li, S. Savarese, M. Savva, S. Song, H. Su, J. Xiao, L. Yi, and F. Yu. Shapenet: An information-rich 3d model repository. *CoRR*, abs/1512.03012, 2015.
[21] M. Chang, J. Lambert, P. Sangkloy, J. Singh, S. Bak, A. Hartnett, D. Wang, P. Carr, S. Lucey, D. Ramanan, and J. Hays. Argoverse: 3d tracking and forecasting with rich maps. In *CVPR*, pages 8748–8757, 2019.
[22] L. Chen, G. Cong, X. Cao, and K. Tan. Temporal spatial-keyword top-k publish/subscribe. In *ICDE*, pages 255–266, 2015.
[23] L. Chen, S. Shang, C. Yang, and J. Li. Spatial keyword search: a survey. *GeoInformatica*, 24(1):85–106, 2020.
[24] Y. Chen, F. He, Y. Wu, and N. Hou. A local start search algorithm to compute exact Hausdorff Distance for arbitrary point sets. *Pattern Recognition*, 67:139–148, 2017.
[25] F. M. Choudhury, J. S. Culpepper, T. K. Sellis, and X. Cao. Maximizing bichromatic reverse spatial and textual k nearest neighbor queries. *PVLDB*, 9(6):456–467, 2016.
[26] A. Corral, Y. Manolopoulos, Y. Theodoridis, and M. Vassilakopoulos. Closest pair queries in spatial databases. In *SIGMOD*, pages 189–200, 2000.
[27] P. A. de Fernandes Vasconcelos, W. de Sousa Alencar, V. H. da Silva Ribeiro, N. Ferreira Rodrigues, and F. de Gomes Andrade. Enabling spatial queries in open government data portals. In *EGOVIS*, pages 64–79, 2017.
[28] A. Degbelo and B. B. Teka. Spatial search strategies for open government data: A systematic comparison. In *GIR*, pages 1–10, 2019.
[29] Y. Dong, P. Indyk, I. Razenshteyn, and T. Wagner. Learning Space Partitions for Nearest Neighbor Search. In *ICLR*, 2020.
[30] P. Frontiera, R. Larson, and J. Radke. A comparison of geometric approaches to assessing spatial similarity for GIR. *International Journal of Geographical Information Science*, 22(3):337–360, 2008.
[31] Y. Gao, M. Wang, R. Ji, X. Wu, and Q. Dai. 3-D object retrieval with hausdorff distance learning. *IEEE Transactions on Industrial Electronics*, 61(4):2088–2098, 2014.
[32] S. Gupta, R. Kumar, K. Lu, B. Moseley, and S. Vassilvitskii. Local search methods for k-means with outliers. *PVLDB*, 10(7):757–768, 2017.
[33] R. H. Guting, T. Behr, and J. Xu. Efficient k -Nearest Neighbor Search on Moving Object Trajectories. *VLDBJ*, 29(5):687–714, 2010.
[34] A. Guttman. R-trees: A dynamic index structure for spatial searching. In B. Yormark, editor, *SIGMOD'84, Proceedings of Annual Meeting, Boston, Massachusetts, USA, June 18-21, 1984*, pages 47–57, 1984.
[35] A. Guttman. R-trees: a dynamic index structure for spatial searching. *ACM SIGMOD Record*, 14(2):47–57, 1984.
[36] R. Hariharan, B. Hore, C. Li, and S. Mehrotra. Processing spatial-keyword (SK) queries in geographic information retrieval (GIR) systems. In *SSDBM*, page 16, 2007.
[37] T. A. Hoang-Vu, H. T. Vo, and J. Freire. A unified index for spatio-temporal keyword queries. In *CIKM*, pages 135–144, 2016.
[38] R. Krajewski, J. Bock, L. Kloeker, and L. Eckstein. The highd dataset: A drone dataset of naturalistic vehicle trajectories on german highways for validation of highly automated driving systems. In *2018 21st International Conference on Intelligent Transportation Systems (ITSC)*, pages 2118–2125, 2018.
[39] R. R. Larson. Ranking approaches for GIR. *SIGSPATIAL Special*, 3(2):37–41, 2011.
[40] G. Li, J. Feng, and J. Xu. DESKS: direction-aware spatial keyword search. In *ICDE*, pages 474–485, 2012.
[41] P. Li, H. Dai, J. Sun, S. Wang, W. Yang, and G. Yang. EDSS: an exemplar dataset search service over encrypted spatial datasets. In *ICWS*, pages 1344–1346. IEEE, 2024.
[42] P. Li, H. Dai, S. Wang, W. Yang, and G. Yang. Privacy-preserving spatial dataset search in cloud. In *CIKM*, pages 1245–1254, 2024.
[43] T. Li, Q. Pan, L. Gao, and P. Li. A novel simplification method of point cloud with directed Hausdorff distance. In *CSCWD*, pages 469–474, 10 2017.
[44] D. Mottin, M. Lissandrini, Y. Velegrakis, and T. Palpanas. Exemplar Queries: Give me an Example of What You Need. *PVLDB*, 7(5):365–376, 2014.
[45] N. Nandan. A grid-based approach for similarity mining of massive geospatial trajectories. In *CIT*, pages 765–768, 2014.
[46] S. Nutanong, E. H. Jacox, and H. Samet. An incremental Hausdorff distance calculation algorithm. *PVLDB*, 4(8):506–517, 2011.
[47] S. Nutanong and H. Samet. Memory-efficient algorithms for spatial network queries. In *ICDE*, pages 649–660. IEEE Computer Society, 2013.
[48] S. M. Omohundro. Five Balltree Construction Algorithms. Technical report, 1989.
[49] G. H. Orair, C. H. C. Teixeira, W. Meira, Y. Wang, and S. Parthasarathy. Distance-Based Outlier Detection: Consolidation and Renewed Bearing. *PVLDB*, 3(2):1469–1480, 2010.
[50] A. Papadopoulos and Y. Manolopoulos. Multiple range query optimization in spatial databases. In *Advances in Databases and Information Systems*, volume 1475 of *Lecture Notes in Computer Science*, pages 71–82. Springer, 1998.
[51] S. Patro and K. K. Sahu. Normalization: A preprocessing stage. *arXiv preprint arXiv:1503.06462*, 2015.
[52] J. Peng, H. Wang, J. Li, and H. Gao. Set-based similarity search for time series. In *SIGMOD*, pages 2039–2052, 2016.
[53] J. Qi, G. Liu, C. S. Jensen, and L. Kulik. Effectively Learning Spatial Indices. *PVLDB*, 13(11):2341–2354, 2020.
[54] B. Qiao, B. Hu, J. Zhu, G. Wu, C. G. Giraud-Carrier, and G. Wang. A top-k spatial join querying processing algorithm based on spark. *Inf. Syst.*, 87, 2020.
[55] E. K. Rezig, A. Bhandari, A. Fariha, B. Price, A. Vanterpool, V. Gadepally, and M. Stonebraker. Dice: Data discovery by example. *PVLDB*, 14(12):2819–2822, 2021.
[56] V. Satopää, J. Albrecht, D. Irwin, and B. Raghavan. Finding a "Kneedle" in a Haystack: Detecting Knee Points in System Behavior. In *ICDCS Workshops*, pages 166–171, 2011.
[57] S. Sieranoja and P. Fränti. Constructing a high-dimensional *k*nn-graph using a z-order curve. *ACM J. Exp. Algorithmics*, 23, 2018.
[58] R. F. Sproull. Refinements to nearest-neighbor searching in k-dimensional trees. *Algorithmica*, 6(4):579–589, 1991.
[59] A. A. Taha and A. Hanbury. An Efficient Algorithm for Calculating the Exact Hausdorff Distance. *IEEE Transactions on Pattern Analysis and Machine Intelligence*, 37(11):2153–2163, 11 2015.
[60] L. Tran, L. Fan, and C. Shahabi. Distance-based Outlier Detection in Data Streams. *PVLDB*, 9(12):1089–1100, 2016.
[61] L. Tran, M. Y. Mun, and C. Shahabi. Real-time distance-based outlier detection in data streams. *PVLDB*, 14(2):141–153, 2020.
[62] H. Wang, X. Fu, J. Xu, and H. Lu. Learned index for spatial queries. In *MDM*, pages 569–574, 2019.
[63] J. Wang and Y. Tan. Hausdorff distance with k-nearest neighbors. In *ICSI*, pages 272–281, 2012.
[64] M. Wang, H. Ma, S. Guan, Y. Bian, H. Che, A. Daundkar, A. Sehirlioglu, and Y. Wu. Modsnet: Performance-aware top-k model search using exemplar datasets. *Proc. VLDB Endow.*, 17(12):4457–4460, 2024.
[65] S. Wang, Z. Bao, J. S. Culpepper, T. Sellis, M. Sanderson, and X. Qin. Answering top-k exemplar trajectory queries. In *ICDE*, pages 597–608, 2017.
[66] S. Wang, Z. Bao, J. S. Culpepper, Z. Xie, Q. Liu, and X. Qin. Torch: A search engine for trajectory data. In *SIGIR*, pages 535–544, 2018.
[67] S. Wang, Z. Bao, S. Huang, and R. Zhang. A unified processing paradigm for interactive location-based web search. In *WSDM*, pages 601–609, 2018.
[68] C. Winter, A. Kipf, T. Neumann, and A. Kemper. GeoBlocks: A Query-Driven Storage Layout for Geospatial Data. In *EDBT*, pages 169–180, 2021.
[69] C. Xiao, W. Wang, X. Lin, J. X. Yu, and G. Wang. Efficient similarity joins for near-duplicate detection. *TODS*, 36(3):15:1–15:41, 2011.
[70] W. Yang, S. Wang, Y. Sun, and Z. Peng. Fast dataset search with earth mover's distance. *Proc. VLDB Endow.*, 15(11):2517–2529, 2022.
[71] Z. Yang, B. Zheng, G. Li, N. Q. V. Hung, G. Liu, and K. Zheng. Searching activity trajectories by exemplar. *Trans. Data Sci.*, 1(3):19:1–19:18, 2020.
[72] Z. Yao, Y. Fu, B. Liu, Y. Liu, and H. Xiong. Poi recommendation: A temporal matching between poi popularity and user regularity. In *ICDM*, pages 549–558,

2016.
[73] J. X. Yew, N. Liao, D. Mo, and S. Luo. Example searcher: A spatial query system via example. In *ICDE*, pages 3635–3638, 2023.
[74] H. Yin, W. Wang, H. Wang, L. Chen, and X. Zhou. Spatial-aware hierarchical collaborative deep learning for POI recommendation. *IEEE Trans. Knowl. Data Eng.*, 29(11):2537–2551, 2017.
[75] C. Yu, B. Cui, S. Wang, and J. Su. Efficient index-based KNN join processing for high-dimensional data. *Inf. Softw. Technol.*, 49(4):332–344, 2007.
[76] J. Yuan, Y. Zheng, C. Zhang, W. Xie, X. Xie, G. Sun, and Y. Huang. T-drive: Driving directions based on taxi trajectories. In *GIS*, pages 99–108, 2010.
[77] E. T. Zacharatou, H. Doraiswamy, A. Ailamaki, C. T. Silva, and J. Freire. GPU rasterization for realtime spatial aggregation over arbitrary polygons. *PVLDB*, 11(3):352–365, 2017.
[78] E. T. Zacharatou, D. Šidlauskas, F. Tauheed, T. Heinis, and A. Ailamaki. Efficient bundled spatial range queries. In *SIGSPATIAL*, pages 139–148, 2019.
[79] S. Zhang, S. Ray, R. Lu, and Y. Zheng. Spatial interpolation-based learned index for range and knn queries. *CoRR*, abs/2102.06789, 2021.
[80] Y. Zhao, Z. Nasrullah, and Z. Li. Pyod: A python toolbox for scalable outlier detection. *Journal of Machine Learning Research*, 20(96):1–7, 2019.
[81] K. Zheng, Y. Zheng, N. J. Yuan, S. Shang, and X. Zhou. Online discovery of gathering patterns over trajectories. *IEEE Trans. Knowl. Data Eng.*, 26(8):1974–1988, 2014.
[82] Y. Zhong, J. Li, and S. Zhu. Continuous spatial keyword search with query result diversifications. *World Wide Web (WWW)*, 26(4):1935–1948, 2023.
[83] J. Zhou, A. K. H. Tung, W. Wu, and W. S. Ng. A "semi-lazy" approach to probabilistic path prediction. In *SIGKDD*, pages 748–756. ACM, 2013.
[84] A. Zomorodian and H. Edelsbrunner. Fast Software for Box Intersections. In *SCG*, pages 129–138, 2000.

9 Appendix

9.1 Notations

Frequently used notations are summarized in Table 3.

Table 3: Summary of notations.

Notation	Description
$p, D, \mathcal{D}$	a data point, a dataset and a data repository
d	the dimension of spatial data point
$\|D\|$	the number of spatial points in the dataset $\|D\|$
$\|\mathcal{D}\|$	the number of datasets in the data repository $\|\mathcal{D}\|$
R, Q	a query range and a query dataset
$b^{\downarrow}, b^{\uparrow}$	the bottom left corner and upper right corner of the minimum bounding rectangle (MBR) of the dataset
$2^{\theta}, \theta$	the number of cells in each dimension, resolution
$z(D)$	the z-order signature of dataset D
N_D	a dataset root node corresponding to the dataset D
o, r	center point and radius of index node
N_l, N_r	left and right child nodes of index node
f	the leaf nodes' capacity
ϕ	a sorted list to store all leaf nodes' radii
ϵ	the threshold parameter for approximate Hausdorff

9.2 Time Complexity Analysis

We use n to represent the number of points in each dataset, and m to represent the number of datasets in the data repository. The construction of the unified index involves both the construction of the bottom-level index and the upper-level index. In constructing the bottom-level index for each dataset. Algorithm 1 first splits the data points into two child sets from which trees are recursively built. During each splitting step, the time complexity for splitting all data points is $O(n)$, and the height of the bottom-level index is $\log(n)$. Thus, the time complexity is $O(n \log n)$.

For outlier removal, the bottom-level index needs to sort the radii of all leaf nodes and compute the radius threshold r', resulting in a time complexity of $O(n \log n)$. Finally, the bottom-level index traverses up from all leaf nodes to remove those potential outliers and refine the dataset index node, resulting in a time complexity of $O(2n)$. Thus, the total time complexity of the bottom-level index for each dataset is $O(n \log n + n \log n + 2n) = O(n \log n)$.

In contrast, the construction process of the upper-level follows a similar approach to that of the bottom-level index, yielding a time complexity of $O(m \log m)$. Since the number of datasets m is significantly smaller than the number of data points n in each dataset D, m can be considered negligible in comparison to n. Thus, the total time complexity of constructing the unified index is $O(m \log m + m(O(n \log n))) = O(mn \log n)$.

9.3 Additional Experimental Results

Effect of High-dimensional Dataset. To investigate the scalability of our proposed index, we also conduct experiments to demonstrate the construction cost and search performance of our proposed unified index and algorithm on high-dimensional datasets. Here, we utilize the highD dataset [38], a large-scale 25-dimensional user trajectories dataset collected from German highways. The highD dataset is publicly available online[3]. Additionally, comprehensive details on the dataset format and column descriptions are provided[4].

Specifically, we first compare the construction cost on the highD data repository between our unified index and the independent index [46] of IncHaus. Figure 24 shows the index construction time comparison of two indexes as the data repository scale m increases. We can see that the construction time for both indexes rises as the data repository scale m increases, which is expected, as larger m imposes greater computational burdens, further increasing the construction time.

In addition, combined with Figure 26 in Section 7.2, we can observe that the construction time for both indexes is higher on the high-dimensional data repository compared to the low-dimensional one. This is because the increase in dimension leads to a decrease in the efficiency of space partitioning when building a tree. However, our proposed unified index still consistently outperforms IncHaus, which achieves at most 23.3% speedup over the index of IncHaus.

Subsequently, we compare the search performance of our ExactHaus and ApproHaus with IncHaus and ScanHaus on the highD data repository as the k increases. The search experimental results are shown in Fig 25. With the increase of k, we can observe that ExactHaus and ApproHaus drastically improve the search performance of the top-k Huasdorff search compared with the other two comparison algorithms, achieving speed improvements of up to several orders of magnitude. This indicates that our algorithms based on the unified index can effectively filter out unpromising datasets even in high-dimensional scenarios. In addition, we can see that the ApproHaus is very fast, completing the search process within one second, which provides faster response time in high-dimensional datasets. Overall, these experimental results verify that our index and search algorithms are very scalable on the high-dimensional spatial data repository.

Comparison of Index and Search Algorithms. To further investigate the efficiency of our proposed framework and algorithms on a specific data repository at a more granular level, we added an experiment to compare the time cost of constructing the integrated index and dataset search and data point search in the **Chicago** data repository. Firstly, we present the experimental results of the dataset search using multiple similarity metrics, including RangeS, IA, GBO, and ExactHaus. In contrast, in the data point search, we provided the experimental results of RangeP and NNP.

From Figure 26 we can observe that as the data repository scale m increases, the running time of index construction and dataset search algorithm gradually increases, while the running time of data point search does not significantly change. This is because the data point search defined in Section 3.4 is between the query dataset and the specified result dataset, which is not affected by the scale of the data repository.

Additionally, we can also see that with the increase of m, the running time of ExactHaus search is longer compared to the other search methods. This is due to the fact that the Hausdroff distance

[3]The highD dataset is available online: https://levelxdata.com/highd-dataset/

[4]The dataset format information can be found at: https://levelxdata.com/wp-content/uploads/2023/10/highD-Format.pdf.

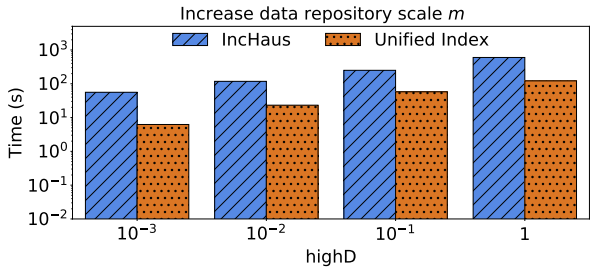

Figure 24: Index's construction time with increasing data repository scale $m = \{10^{-3}, 10^{-2}, 10^{-1}, 1\} \times |\mathcal{D}|$.

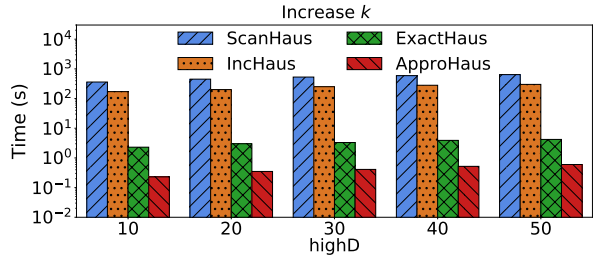

Figure 25: Top-k Hausdorff search with increasing k.

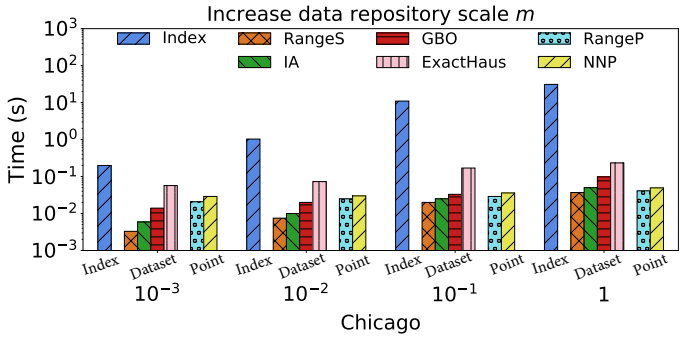

Figure 26: Index's construction time and the search time of dataset search and data point search with increasing scale m in Chicago data repository.

requires the computation of pairwise point distance, which consumes a lot of time. However, the running time still remains under one second, demonstrating the effectiveness of the index-based acceleration algorithm we have designed.